Int J Clin Exp Pathol 2013;6(8):1493-1504
www.ijcep.com /ISSN:1936-2625/IJCEP1306018

Original Article

RAF1-MEK1-ERK/AKT axis may confer NSCLC cell lines resistance to erlotinib

Zhi-Hong Xu[1], Jun-Biao Hang[2], Jia-An Hu[1], Bei-Li Gao[3]

[1]Department of Geriatrics, Ruijin Hospital affiliated to Shanghai JiaoTong University, Shanghai, China; [2]Department of Thoracic surgery, Ruijin Hospital affiliated to Shanghai JiaoTong University, Shanghai, China; [3]Department of Respiratory, Ruijin Hospital affiliated to Shanghai JiaoTong University, Shanghai, China

Received June 20, 2013; Accepted July 5, 2013; Epub July 15, 2013; Published August 1, 2013

Abstract: The fact that advanced NSCLC patients with wild type (wt) EGFR can benefit from erlotinib therapy makes it critical to find out biomarkers for effective selection of patients and improving the therapy effects. In present study, 3 NSCLC cell lines (U1752, Calu-6 and NCI-H292) with wt EGFR and different sensitivities to erlotinib were used for microarray analysis. The differential basal gene expression between 2 NSCLC cell lines was analyzed, about 353 genes were expression-altered with higher than 2-fold changes between Calu-6 and U1752. And Ingenuity Pathway Analysis (IPA) showed that these genes were mainly enriched in regulation of epithelial–mesenchymal transition (EMT) pathway, Wnt-β catenin signaling, Tec kinase signaling and some types of cancer-related signaling. More interestingly, RAF1 (c-raf), MAP2K1 (MEK1), SNAI and downstream signaling molecules ERK and AKT were predicted to be activated in erlotinib-resistant cell line by IPA. Subsequent immunoblotting experiments showed that the phosphorylation of ERK and AKT were exactly increased stepwise from erlotinib sensitive cell line to erlotinib resistant cell lines. Collectively, activation of RAF1-MEK1-ERK/AKT axis may determine the resistance of NSCLC cell lines bearing wt EGFR to erlotinib. Our work provides potential biomarkers and therapeutic targets for NSCLC patients harboring wt EGFR.

Keywords: Non-small cell lung cancer, NSCLC, EGFR, erlotinib, microarray, RAF1, MAP2K1, ERK, AKT

Introduction

Erlotinib, a small-molecule drug targeted to the tyrosine kinase activity of EGFR, is approved by FDA to treat advanced or metastatic non-small cell lung cancer (NSCLC) and pancreatic cancer that cannot be removed by surgery or has metastasized. Clinical trials and preclinical studies have suggested that EGFR activating mutation is a predictive marker for favorable outcome of erlotinib in NSCLC patients [1-3]. Recently, first-line erlotinib therapy in EGFR mutation-positive NSCLC patients showed profound advantage over chemotherapy in the objective response rate and progression-free survival (PFS) benefit [4, 5]. However, only 10-30% of NSCLC patients harbor mutant EGFR [6-8], the majority of NSCLC patients are with wild type (wt) EGFR. There also appear to be NSCLC patients with wt EGFR who clinically benefit from erlotinib therapy by stabilizing disease and preventing further progression [1, 9, 10]. However, the mechanism of this benefit remains largely unknown and the biomarkers for wt EGFR NSCLC patients who can derive benefit from erlotinib treatment need to be further uncovered.

One possible mechanism that influences the sensitivity of wt EGFR NSCLC cells to erlotinib is in the driver gene alterations other than EGFR mutation, such as gene mutation (e.g. KRAS, HER2, BRAF), gene amplification (e.g. MET, FGFR1) or gene translocation (e.g. ALK, ROS1, RET). Various studies suggest that these driver gene alterations play roles in erlotinib resistance in NSCLC cells [11-13]. For example, MET activation and amplification was recently proposed to be linked closely to erlotinib resistance [13, 14]. However, most of the currently known driver mutations occur at an incidence of ≤5%. The incidences of mutations in lung cancer were as follows: KRAS 25%, BRAF 3%, HER 21%, MET amplifications 2%, and ALK rear-

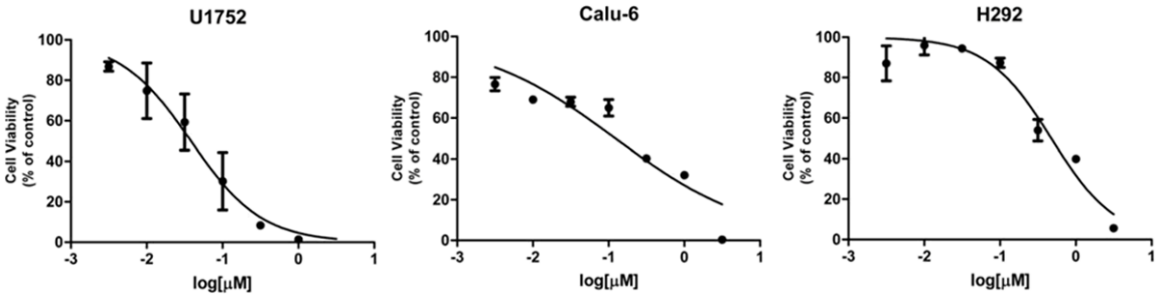

Figure 1. 3 NSCLC cell lines display different sensitivities to erlotinib. U1752, Calu-6 and NCI-H292 cells were administrated to 7 concentrations of erlotinib (0, 0.0032, 0.01, 0.032, 0.10, 0.32, 1.00, 3.20 μmol/L, respectively) for 72 h. The cell viability was determined by MTS assay. Every treatment was triplicate in the same experiment. Bars represent the standard errors.

Table 1. Top 20 significantly expression-altered genes in Calu-6 compared to U1752

Gene Symbol	fold change	*P* value	Description
FABP4	6.49	2.29E-03	fatty acid binding protein 4, adipocyte
TIMP3	6.29	6.80E-04	TIMP metallopeptidase inhibitor 3
CDK15	5.63	3.55E-04	cyclin-dependent kinase 15
TGFBI	5.60	4.46E-04	transforming growth factor, beta-induced, 68 kDa
EMP1	5.23	6.63E-04	epithelial membrane protein 1
THBS1	4.91	3.31E-05	thrombospondin 1
NT5E	4.67	7.40E-06	5'-nucleotidase, ecto (CD73)
RGS1	4.67	8.63E-04	regulator of G-protein signaling 1
IGFBP5	4.38	8.98E-04	insulin-like growth factor binding protein 5
SERPINF1	4.29	1.37E-03	serpin peptidase inhibitor, clade F (alpha-2 antiplasmin, pigment epithelium derived factor), member 1
GRAMD1B	0.24	7.15E-04	GRAM domain containing 1B
HIST1H3I	0.24	4.36E-04	histone cluster 1, H3i
FAM5C	0.23	1.93E-04	family with sequence similarity 5, member C
HSPA13	0.21	4.90E-04	heat shock protein 70 kDa family, member 13
OSMR	0.21	1.59E-03	oncostatin M receptor
NTS	0.19	1.88E-04	neurotensin
CYP24A1	0.18	1.88E-05	cytochrome P450, family 24, subfamily A, polypeptide 1
INA	0.18	7.36E-04	internexin neuronal intermediate filament protein, alpha
EDIL3	0.16	7.84E-04	EGF-like repeats and discoidin I-like domains 3
TFPI2	0.11	5.08E-06	tissue factor pathway inhibitor 2

rangements 6% [15, 16]. Although KRAS mutation frequency is relative high in lung cancer, in vitro data show various degrees of sensitivity to erlotinib in KRAS-mutated NSCLC cell lines [17, 18]. Moreover, clinical trial showed that KRAS mutation has no significant effect on PFS of erlotinib treatment in NSCLC patients [1]. So, driver gene alterations may confer sensitivity/resistance to erlotinib only in a small part of patients, there must be other mechanisms by which cancer cells bearing wt EGFR displayed distinct sensitivity to erlotinib.

Several reports suggested that the expression of epithelial to mesenchymal transition (EMT)-related genes mediated NSCLC and head and neck squamous cell carcinoma cells sensitivity to erlotinib or gefitinib, another small molecule drug of EGFR tyrosine kinase inhibitor (TKI) [17, 19, 20]. Increased expression of TGF-β, IL6 and Vimentin was observed in erlotinib resistant NSCLC cell lines, while E-cadherin was up-regulated in sensitive cell lines [19]. Furthermore, Balko et al proposed that expression of genes linked to signal transduction (NF-κB signaling

Table 2. IPA for 353 genes expression-altered significantly in Calu-6 compared to U1752

Ingenuity Canonical Pathways	*P* value	Molecules
Hepatic Fibrosis/Hepatic Stellate Cell Activation	9.77E-07	TGFBR2, TLR4, IGFBP4, FN1, CCL2, HGF, TGFB2, TGFA, LAMA1, MMP2, IGFBP5, A2M, TNFRSF11B
Regulation of the Epithelial-Mesenchymal Transition Pathway	7.94E-05	TGFBR2, TCF4, CDH12, SNAI2, HGF, TGFB2, mir-155, MMP2, WNT2, HMGA2, FZD7, FGF5
Wnt/β-catenin Signaling	8.32E-04	TGFBR2, MYC, GJA1, TCF4, CDH12, FRZB, CD44, TGFB2, WNT2, FZD7
Colorectal Cancer Metastasis Signaling	1.00E-03	TGFBR2, MYC, TLR4, GNB4, TCF4, RND3, TGFB2, MMP2, PTGS2, GNG2, WNT2, FZD7
LPS/IL-1 Mediated Inhibition of RXR Function	1.66E-03	TLR4, MGST1, SULT1C2, ACSL5, FABP4, HS6ST3, CHST10, FABP3, ALDH7A1, TNFRSF11B, PPARGC1A
Epithelial Adherens Junction Signaling	3.98E-03	TGFBR2, TCF4, SNAI2, HGF, PVRL3, CTNNA1, TGFB2, JUP
Inhibition of Matrix Metalloproteases	4.68E-03	TIMP3, MMP2, A2M, TFPI2
Thyroid Cancer Signaling	5.13E-03	PPARG, MYC, TCF4, BDNF
LXR/RXR Activation	5.37E-03	TLR4, CCL2, SERPINF1, CLU, PTGS2, PON3, TNFRSF11B
Polyamine Regulation in Colon Cancer	6.31E-03	PPARG, MYC, TCF4
Role of Macrophages, Fibroblasts and Endothelial Cells in Rheumatoid Arthritis	6.76E-03	MYC, TLR4, TCF4, FN1, FRZB, CCL2, LTBR, IRAK3, WNT2, PRKD1, FZD7, TNFRSF11B
Chondroitin Sulfate Biosynthesis (Late Stages)	7.76E-03	SULT1C2, HS6ST3, CHST10, CSGALNACT1
Ovarian Cancer Signaling	8.51E-03	GJA1, TCF4, CD44, MMP2, PTGS2, WNT2, FZD7
RhoGDI Signaling	1.07E-02	GNB4, CDH12, RND3, CDH10, CD44, CDH6, GNG2, GNAL
Chondroitin Sulfate Biosynthesis	1.38E-02	SULT1C2, HS6ST3, CHST10, CSGALNACT1
Dermatan Sulfate Biosynthesis	1.55E-02	SULT1C2, HS6ST3, CHST10, CSGALNACT1
Molecular Mechanisms of Cancer	1.62E-02	TGFBR2, MYC, RASGRF2, TCF4, RND3, CTNNA1, CDK6, TGFB2, BIRC3, GNAL, PRKD1, FZD7
Glioma Invasiveness Signaling	1.74E-02	TIMP3, RND3, CD44, MMP2

cascade and PI3K/MAPK pathway) may serve as predictive markers for erlotinib sensitivity in NSCLC cell lines and patients with lung adenocarcinomas [21]. Moreover, the protein expression of EGFR [1], amphiregulin [22], HGF [13] and cyclin D3 [23] was implicated in erlotinib sensitivity in vitro or in vivo, whether the mRNA expression of these genes is related to erlotinib sensitivity is not yet well defined.

In present study, 3 NSCLC cell lines with different sensitivities to erlotinib were applied to gene expression profile analysis. The differentially expressed genes were validated by quantitative real-time PCR. The potential genes/pathways involved in erlotinib sensitivity were proposed.

Materials and methods

Cell culture

U1752, Calu6 and H292 cell lines were purchased from ATCC and maintained in DMEM or RPMI 1640 medium supplemented with 10% FBS (Hyclone), penicillin (100 IU/ml) and Streptomycin (100 μg/ml) (Life Technologies).

MTS assay for 3 NSCLC cell lines viability

Cells (4×10^3) were grown in 100 μl of DMEM or RPMI 1640medium containing serum per well in a 96-well plate. After 24 h, the cells were treated with erlotinib (0, 0.0032, 0.01, 0.032, 0.10, 0.32, 1.00, 3.20 μmol/L, respectively) for 72 h. Every treatment was triplicate in the same experiment. Then 20 μl of MTS (CellTiter 96 AQueous One Solution Reagent; Promega) was added to each well for 2 h at 37°C. After incubation, the absorbance was read at a wavelength of 490 nm according to the manufacturer's protocol. The IC50 calculation was performed with GraphPad Prism 5.0 software.

Microarray analysis

3 NSCLC cell lines (8×10^4) were grown in 2 ml of DMEM medium containing serum per well in

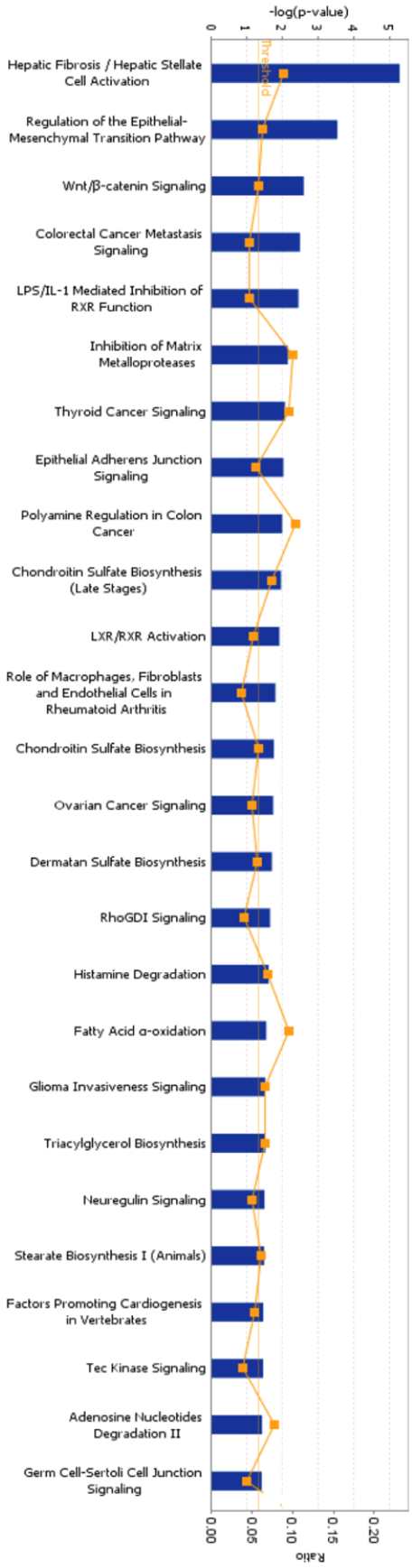

Figure 2. IPA for differentially expressed genes between Calu-6 and U1752. 353 genes whose expression altered by higher than 2-fold in Calu-6 and U1752 were applied to IPA. The canonical pathways ($p < 0.05$) were shown in this figure. The thresh line represents $p = 0.05$. The ratio means the proportion that the amounts of genes involved in some pathway account for the total 353 genes.

a 6-well plate. Cells in the exponential growth phase were used for microarray analysis. Every treatment was duplicated in the same experiment. All the samples were homogenized with 1 ml Trizol (Invitrogen, Life Technologies) and total RNAs were extracted according to the manufacturer's instruction.

500 ng total RNA was used to synthesize double-strand cDNA and in vitro transcribed to cRNA, purified 10 μg cRNA was used to synthesize 2nd-cycle cDNA and then hydrolyzed by RNase H and purified. Above steps were performed with Ambion WT Expression Kit. 5.5 μg 2nd-cycle cDNA was fragmented and the single-stranded cDNA was labeled with GeneChip2 WT Terminal Labeling Kit and Controls Kit (Affymetrix, PN 702880). About 700 ng fragmented and labeled single-stranded cDNA were hybridized to an Affymetrix GeneChip Human Gene 1.0 ST array, which was washed and stained with GeneChip2 Hybridization, Wash and Stain kit (Affymetrix).

Microarray data analysis was done using Significance Analysis of Microarrays (SAM) method, as described before [24]. Functional annotation was performed to the differential expression genes with Ingenuity Pathway Analysis (IPA) online software.

Quantitative real-time PCR (qPCR)

Total RNA above isolated was synthesized to cDNA using PrimeScript RT reagent kit with gDNA Eraser (Takara, RR074A) for RT-PCR with mixture of oligo-dT and Random Primer (9 mer). The primers used for qPCR validation were list in Supplementary Table 1. Real-time qPCR was performed on CFX-96 (Bio-lab), with endogenous control hActb. Gene expression was calculated relative to expression of hActb endogenous control and adjusted relative to expression in U1752 cells.

Protein isolation and western blotting

Cell pellets were resuspended in 1 × SDS loading buffer (1 mmol/L Na_3VO_4, 10 mmol/L NaF, 1 mmol/L PMSF) containing protease inhibitors. Lysates (20 μg each lane) were applied to SDS-PAGE. Immunoblotting of Abs specific for GAPDH (Abmart, 080922), EGFR (Abclonal, A0227), p-EGFR (Santa cruz, SC-12351, pY1173), p-EGFR (Epitomics, #1139-S, pY1086), AKT (Santa Cruz, sc-8312), p-AKT (Santa Cruz, SC-7985-R, pS473), ERK (Abclonal, A0228) and p-ERK (Cell signaling, #9106S,

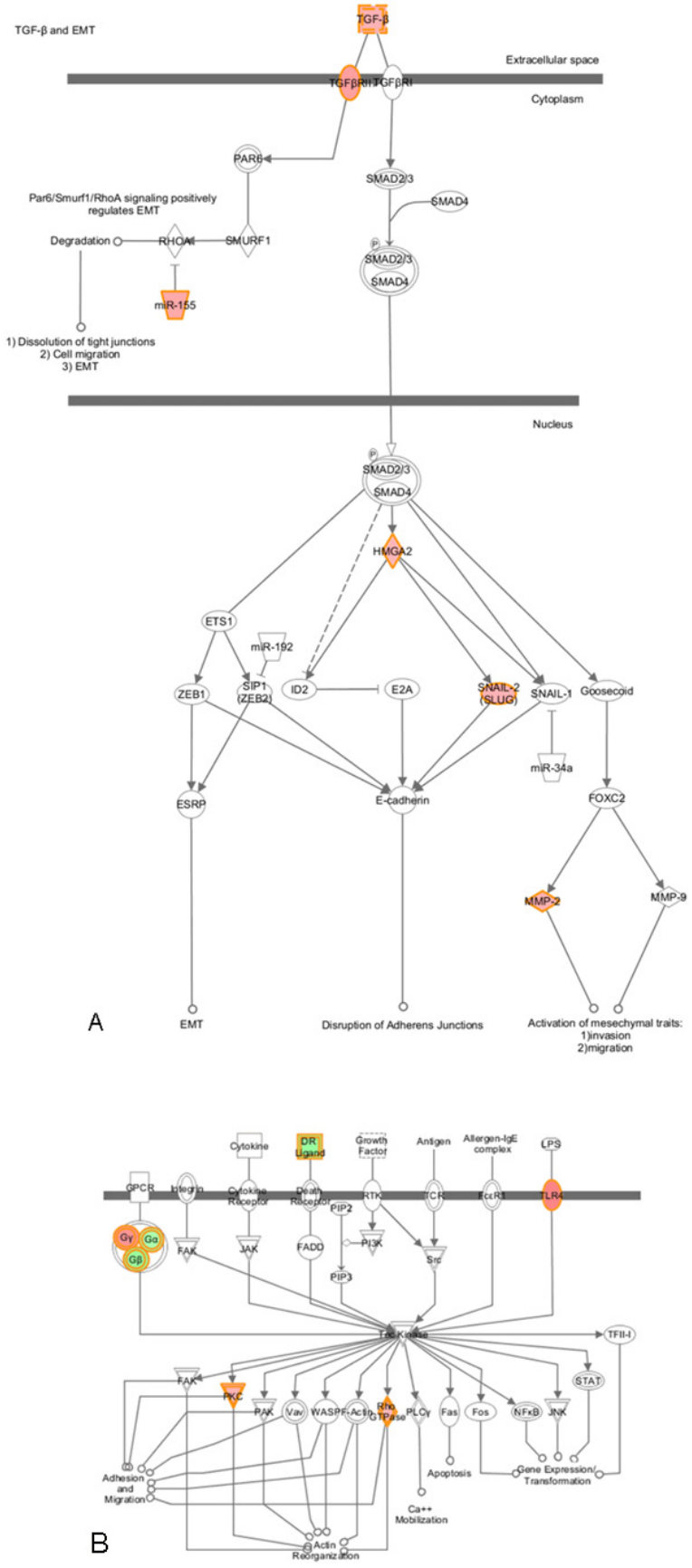

Figure 3. Regulation of the EMT Pathway and Tec kinase signaling in Calu-6 compared to U1752. This figure was derived from IPA. The colored molecules were genes whose expression altered significantly in Calu-6 compared to U1752. The red color represented up-regulated genes in Calu-6, while the green color represented down-regulated genes in Calu-6. A: Regulation of the EMT Pathway in Calu-6 compared to U1752. TGF-β-EMT was shown, while Wnt-EMT, Notch-EMT and Receptor tyrosine kinase-EMT were not shown. B: Tec kinase signaling in Calu-6 compared to U1752.

pT202/204) were detected using HRP-conjugated anti-mouse (Promega) or anti-rabbit (Promega) and visualized by chemiluminescence detection system (Millipore, WBKLS0500).

Statistical analysis

R^2 values were calculated using Pearson's correlation coefficient. The significant difference was calculated using Student's t-test.

Results

3 NSCLC cell lines display distinct sensitivities to erlotinib

Three NSCLC cell lines harboring wt EGFR, U1752, Calu-6 and NCI-H292, were treated with 7 different concentrations of erlotinib as indicated for 72 h. Then the cell viability was determined by MTS assay (**Figure 1**) and IC50 s of these three cell lines were calculated. IC50 dose of U1752, Calu-6 and NCI-H292 cells to erlotinib at 72 h were 0.059 ± 0.029 (R^2 = 0.99), 0.217 ± 0.134 (R^2 = 0.86) and 0.503 ± 0.041 μmol/L (R^2 = 0.95), respectively. According to criterion described before [25],

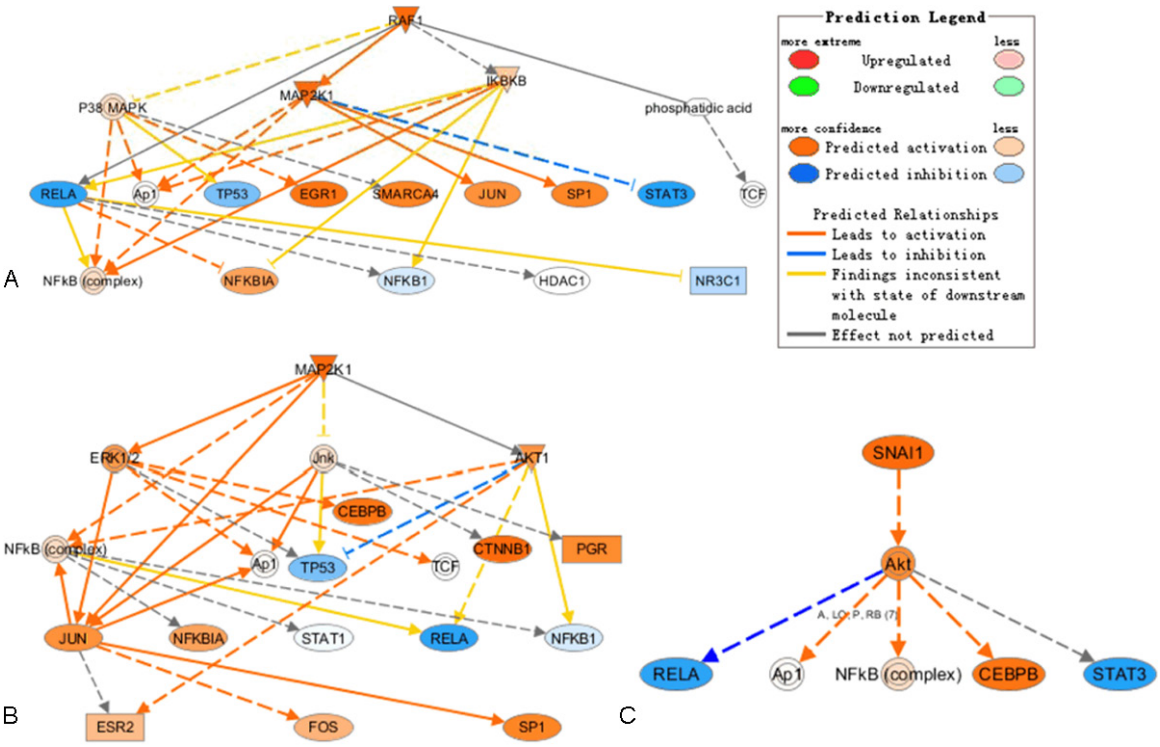

Figure 4. Mechanistic network analysis by IPA in Calu-6 compared to U1752. RAF1 (A), MAP2K1 (B), and SNAI (C) were predicted to be activated. The downstream molecules regulated by RAF1, MAP2K1, and SNAI and interactions between these molecules were illustrated.

U1752 was sensitive to erlotinib whereas Calu-6 and NCI-H292 were relatively insensitive to erlotinib.

Differential gene expression profile analysis

To figure out the biomarkers that determine the different sensitivities to erlotinib, the 3 NSCLC cell lines were applied to microarray analysis. The raw data of microarray showed that there was dramatically difference in basal expression between U1752 and Calu-6 cells. 1163 genes were up-regulated by 2-fold and 1378 genes were down-regulated by 2-fold in Calu-6 compared to U1752 (data not shown). The most markedly expression-altered genes were TIMP3 and TFPI2, the expression of TIMP3 was increased by 191-fold and that of TEPI2 was decreased by 411-fold in Calu-6 compared to U1752, respectively. However, limited alterations were observed in basal expression between U1752 and NCI-H292 cells. Expression of only one gene (CDKN2AIPNLP1) and two genes (OR4A47 and WT1-AS) was increased and decreased by 2-fold, respectively, in NCI-H292 compared to U1752. There were no genes whose expression was increased or decreased by higher than 50% stepwise from U1752 to Calu-6 to NCI-H292, according to their sensitivities to erlotinib. These results suggested that the relative resistance of Calu-6 and NCI-H292 to erlotinib may be caused by different mechanisms; the resistance of NCI-H292 to erlotinib may be not explained by gene expression.

Then we analyzed the microarray data of Calu-6 and U1752 by SAM method. The results showed that 177 genes and 176 genes were respectively up-regulated and down-regulated by higher than 2-fold in Calu-6 compared to U1752 (Supplementary Table 2). Interestingly, EREG (epiregulin), a ligand of EGFR, was up-regulated by 2.2-fold in Calu-6 compared to U1752. The top 20 significantly expression-altered genes were list in **Table 1**. Within these genes, TIMP3, CDK15, TGFBI and IGFBP5 were up-regulated, while HIST1H3I, HSPA13 and CYP24A1 were down-regulated.

The 353 genes (177 up-regulated genes and 176 down-regulated genes) were applied to IPA. These genes were mainly enriched in regulation of epithelial–mesenchymal transition (EMT)

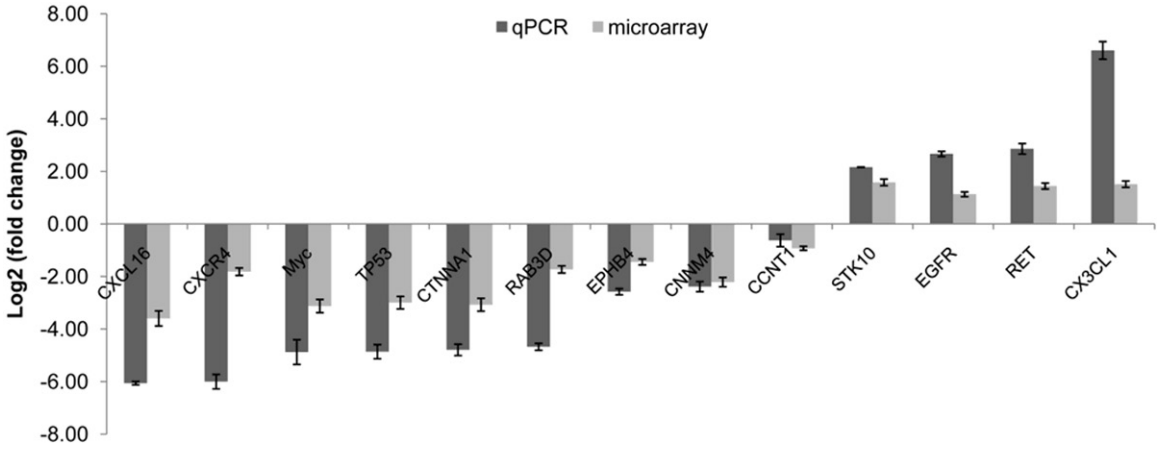

Figure 5. qPCR validation for microarray data. 13 genes were selected to perform qPCR. The expression was calculated relative to expression in U1752. The change folds determined by qPCR and microarray were transformed to log2. Bars represent the standard errors.

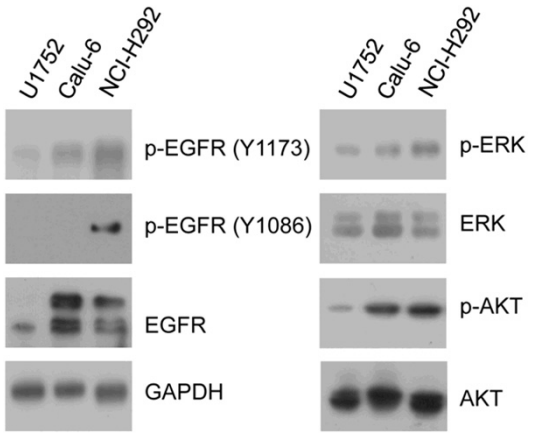

Figure 6. The activation status of EGFR/ERK/AKT in 3 NSCLC cell lines. U1752, Calu-6 and NCI-H292 cells were applied to western blotting for EGFR, p-EGFR (Y1173), p-EGFR (Y1086), ERK, p-ERK (T202/204), AKT, p-AKT (S473). GAPDH was used as input control.

pathway, Wnt-β catenin signaling, Tec kinase signaling and some types of cancer-related signaling (**Table 2** and **Figure 2**). 11 genes were involved in regulation of EMT pathway (**Figure 3A**). Among these genes, TGFB2, TGFBR2, HMGA2, SNAI2, MMP2, TCF4, FZD7 and CDH12 were up-regulated, while Wnt2, HGF and FGF5 were down-regulated. Although expression of 3 upstream genes (Wnt2, HGF and FGF5) was decreased, the other upstream signaling molecules (TGFB2 and TGFBR2) and downstream effectors (SNAI2, MMP2 and CDH12) were up-regulated. This result suggests that EMT-regulation pathway is activated in Calu-6, cell line relatively insensitive to erlotinib, compared to U1752. Additionally, there were 7 genes linked to Tec kinase signaling (**Figure 3B**). Expression of 4 genes (TLR4, GNG2, PRKD1 and RND3) was elevated whereas 3 genes (TNFSF10, GNAL and GNB4) were down-regulated. Furthermore, genes associated to cytokine-cytokine receptor interaction (EGFR, CX3CL1, CXCL16 and CXCR4) were also expression-altered markedly in Calu-6 compared to U1752.

RAF1-MAP2K1 and downstream signaling ERK/AKT were predicted to be activated in erlotinib-resistant NSCLC cell line

In the other hand, mechanistic network analysis of IPA showed that RAF1 (C-RAF, **Figure 4A**), MAP2K1 (MEK1, **Figure 4B**) and SNAI (**Figure 4C**) were predicted to be activated in erlotinib-resistant NSCLC cell line compared to erlotinib-sensitive cell line. The prediction of RAF1 activation was based on that 13 genes in the 353-gene list were regulated by RAF1 and that expression directions of 9 out 13 genes were consistent with RAF1 activation, as described before [26-28] (Supplement Table 3). For example, PTGS2 [26], HMGA2 [27], and RND3 [28] were reported to be up-regulated by RAF1, while in our microarray data these 3 genes were all expression-increased in Calu-6, erlotinib-resistant cell line. This indicated that RAF1 was activated in Calu-6. Based on the same way, MAP2K1 and SNAI were predicted to be activated. Interestingly, the downstream signal-

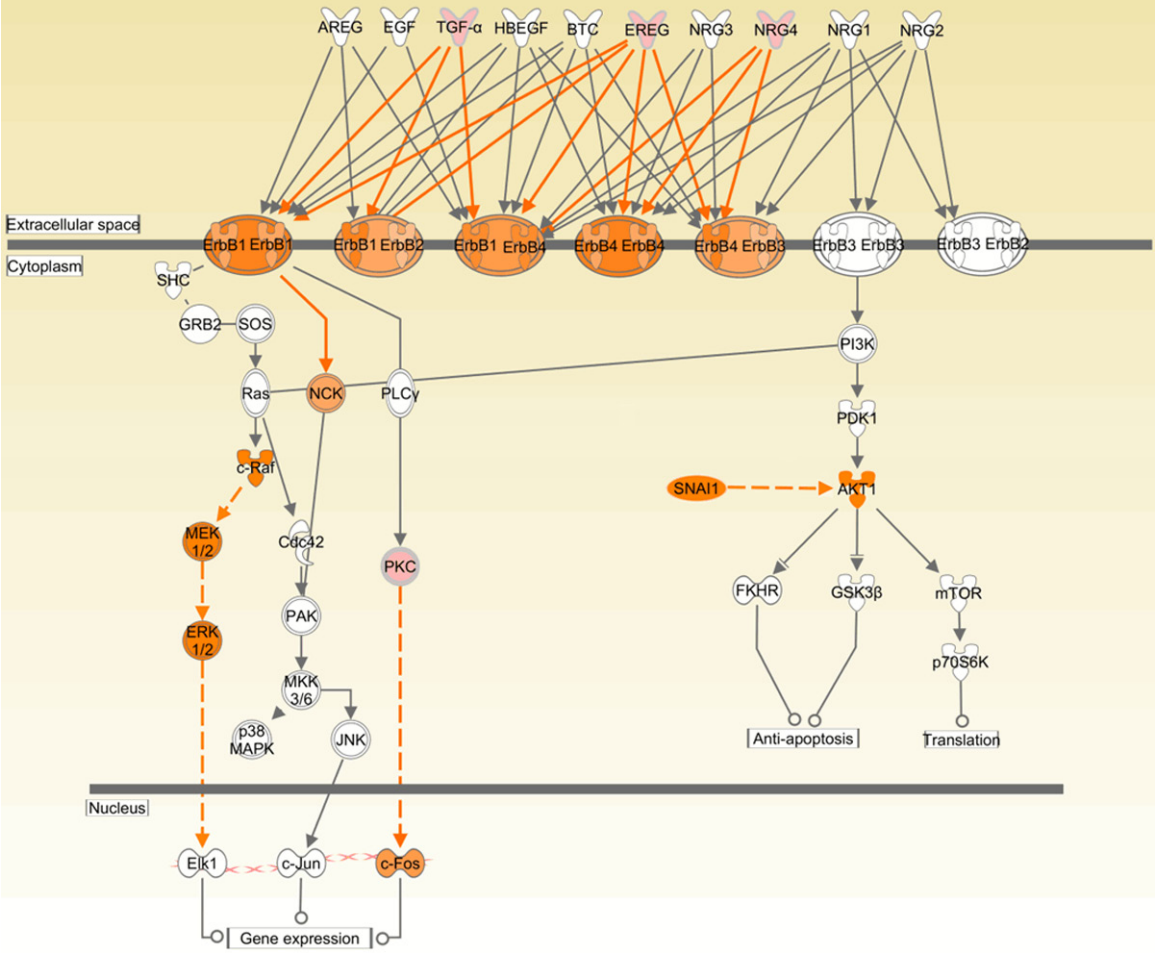

Figure 7. Potential mechanism by which NSCLC cells with wt EGFR display resistance to erlotinib. The up-regulation of ErbB ligands (TGF-α, EREG and NRG4) activates EGFR. Activation of RAF1-MEK1-ERK and PKC/SNAI-AKT up-regulates the downstream signaling and hence confers NSCLC cells harboring wt EGFR resistance to erlotinib. The pink molecules represent that its mRNA expression is up-regulated. The orange molecules mean that it is activated.

ing ERK and AKT were predicted to be activated following RAF1 and MAP2K1 activation.

qPCR validation of microarray data

To validate the microarray data, qPCR was performed for 13 genes whose basal expression altered markedly in Calu-6 compared to U1752. Among these 13 genes, CXCL16 was down-regulated by 67-fold, CXCR4 was down-regulated by 64-fold, Myc and Tp53 were down-regulated by 29-fold, CTNNA1 (α-catenin) was down-regulated by 28-fold, EGFR was up-regulated by 2.7-fold, RET up-regulated by 2.9-fold and CX3CL1 was up-regulated by 6.6-fold. Fold changes of these genes' expression determined by qPCR and microarray were log2 transformed and shown in **Figure 5**. The change folds varied between qPCR and microarray data, however, the expression trends of all the 13 genes were consistent. The correlation between both data sets was examined using R^2 and an R^2 value of 0.93 was obtained, suggesting a strong overall concordance of expression trends between the microarray and qPCR data. The most dramatically expression-altered genes validated by qPCR were CXCL16, CXCR4, Myc, TP53, EGFR, RET and CX3CL1, genes involved in cytokine-cytokine receptor interaction, receptor tyrosine kinase and caner signaling pathways.

ERK and AKT were activated in erlotinib insensitive cell lines

Since expression of EGFR was up-regulated significantly and that ERK and AKT were predicted to be activated in Calu-6 compared to U1752, we next investigated the activation status of EGFR and its downstream signaling ERK and

AKT in the 3 NSCLC cell lines by western blotting (**Figure 6**). The p-EGFR (Y1173) was up-regulated stepwise from U1752 to Calu-6 to NCI-H292, whereas the p-EGFR (Y1086) was detected only in NCI-H292 but not in Calu-6 and U1752. The p-AKT was increased gradually from U1752 to Calu-6 to NCI-H292. The p-ERK was also shown similar pattern among those three cell lines. The protein expression of p-ERK and p-AKT was basically increased from sensitive cell line to insensitive cell lines. Our data suggest that ERK and AKT are highly activated in erlotinib-resistant NSCLC cell lines.

Discussion

The fact that advanced NSCLC patients with wt EGFR can benefit from erlotinib therapy makes it essential to uncover biomarkers for effective selection of patients and improving the therapy. In present study, 3 NSCLC cell lines with wt EGFR and different sensitivities to erlotinib were employed to perform microarray analysis. The differential basal expression between NSCLC cell lines was analyzed and the expression-altered genes were applied to IPA. Expression of 13 genes was validated by qPCR and the activation status of EGFR and its downstream signal ERK/AKT were examined by western blotting.

Since erlotinib is an EGFR tyrosine kinase inhibitor (TKI), EGFR expression level is one of the most frequently mentioned signature for erlotinib sensitivity. However, in this work, the expression of EGFR was as follows: Expression in NCI-H292 was approximately equal to that in U1752 (data not shown), while expression level in Calu-6 was increased by 2.7-fold compared to U1752. This was not in line with erlotinib sensitivities of these cell lines. The subsequent immunoblotting experiments showed that p-EGFR (Y1086) was detectable only in NCI-H292 cell line but not either in U1752 and Calu-6 or in the other two erlotinib-resistant NSCLC cell lines, NCI-H1975 and NCI-H1395 (IC50 dose to erlotinib at 72 h was 0.32 ± 0.09 and 1.49 ± 0.96 μmol/L, respectively; data not shown). Although p-EGFR (Y1086) has been implicated to cancer cells invasion and proliferation [29, 30], it is not likely to be a predictive marker for erlotinib sensitivity, based on our data. At the same time, p-EGFR (Y1173) was up-regulated gradually from erlotinib-sensitive cell line to erlotinib-insensitive cell lines, according to their sensitivities to erlotinib. However, previous reports have suggested that EGFR activation mutation was predictive marker for sensitivity to erlotinib. The aberrant activation of EGFR (Y1173) in cancer cells harboring wt EGFR seems likely to confer resistance to erlotinib. In summary, either mRNA expression of EGFR or p-EGFR (Y1086) may not be potential marker for erlotinib sensitivity in patients harboring wt EGFR.

Activation of bypass pathway or downstream signaling molecules is one of the crucial mechanisms by which cancer cells confer resistance to targeted therapy. For example, constitutive phosphorylation and activation of HER2 and EGFR caused by HER2 kinase domain mutation [11], activating ERBB3 signaling resulted from MET amplification [14], high IκB in NSCLC patients [31] and downstream BRAF activation [12] all confer resistance of cancer cells to EGFR TKI. Recently, a number of studies suggest that the PI3K/Akt signaling pathway is central to NSCLC growth and survival [32-34]. In this work, mechanistic network analysis by IPA predicted that RAF1, MAR2K1, SNAI and downstream signaling ERK/AKT were activated. Although the mRNA expression levels of these 3 genes (RAF1, MAR2K1, SNAI) were not altered significantly (data not shown), the up-regulation of downstream molecules positively regulated by these 3 genes indicated that protein expression levels of these 3 genes were increased. Subsequent immunoblotting experiments validated that p-ERK and p-AKT protein expression increased stepwise from erlotinib sensitive cell line to insensitive cell lines, proposing that p-ERK and p-AKT expression is potential biomarkers for erlotinib resistance and p-ERK and p-AKT may serve as a therapeutic target for combination therapy with EGFR TKI in NSCLC patients bearing wt EGFR. Furthermore, PRKD1, one member of PKC family, was up-regulated in Calu-6 compared to U1752. PRKD1 was proposed to mediate anchorage-dependent and -independent growth of tumor cells via the zinc finger transcription factor Snail1 [35]. The activation of PRKD1 may be another reason that NSCLC cells confer resistance to erlotinib. The possible mechanism of erlotinib resistance in NSCLC cell lines with wt EGFR was illustrated in **Figure 7**.

As for the increased mRNA level of EGFR in Calu-6, it is probable to be illuminated by the up-regulation of ErbB ligands (TGF-α, EREG and NRG4, see in **Figrue 7**) and cytokine (CX3CL1). In our data, TGF-α, EREG, NRG4 and CX3CL1 were up-regulated by 2.2-, 2.2-, 2.1- and 6.6-fold, respectively, in Calu-6 compared to U1752 (Supplementary Table 2 and **Figure 5**). It was reported that CX3CL1 has anti-apoptotic and proliferative effects on human vascular smooth muscle cells via epiregulin-induced EGFR signaling [36], CX3CL1 promotes breast cancer via transactivation of the EGFR pathway [37] and that CX3CL1 induced the phosphorylation and activation of PI3K, AKT and ERK in rheumatoid arthritis fibroblast-like synoviocyte [38] and chronic lymphocytic leukemia cells [39]. So, in some NSCLC cell lines, CX3CL1 may be potential marker for EGFR TKI resistance.

Furthermore, our data also showed that EMT-related pathways were elevated in erlotinib insensitive cell line, which is exactly consistent with previous report [17, 19, 20] and suggests that our microarray data were reliable. Moreover, genes associated to Tec kinase signaling were expression-altered significantly in erlotinib insensitive cell line, indicating that tec kinases may be novel targets for cancer therapy as described before [40, 41].

Taken together, our results present a serial of potential biomarker candidates for further validation in erlotinib sensitivity prediction. And the AKT and EKT hyperphosphorylation contributes to erlotinib resistance might provide the indication of combination with AKT/EKT inhibitor in clinical erlotinib therapy. Moreover, our finding might also suggest a mechanism of secondary drug tolerance in patients treated with erlotinib, although it needs to be addressed more.

Acknowledgments

This work is support by the grant from Health Bureau Research Fund of Shanghai, China (No. 20114291).

Address correspondence to: Dr. Bei-Li Gao and Jia-An Hu, Department of Respiratory and Department of Geriatrics, respectively, Ruijin Hospital affiliated to Shanghai JiaoTong University, Shanghai, China. E-mail: gaobeili_ruijin@163.com; jahu_rj@aliyun.com

References

[1] Brugger W, Triller N, Blasinska-Morawiec M, Curescu S, Sakalauskas R, Manikhas GM, Mazieres J, Whittom R, Ward C, Mayne K, Trunzer K and Cappuzzo F. Prospective molecular marker analyses of EGFR and KRAS from a randomized, placebo-controlled study of erlotinib maintenance therapy in advanced non-small-cell lung cancer. J Clin Oncol 2011; 29: 4113-4120.

[2] Janne PA, Engelman JA and Johnson BE. Epidermal growth factor receptor mutations in non-small-cell lung cancer: implications for treatment and tumor biology. J Clin Oncol 2005; 23: 3227-3234.

[3] Ji H, Li D, Chen L, Shimamura T, Kobayashi S, McNamara K, Mahmood U, Mitchell A, Sun Y, Al-Hashem R, Chirieac LR, Padera R, Bronson RT, Kim W, Janne PA, Shapiro GI, Tenen D, Johnson BE, Weissleder R, Sharpless NE and Wong KK. The impact of human EGFR kinase domain mutations on lung tumorigenesis and in vivo sensitivity to EGFR-targeted therapies. Cancer Cell 2006; 9: 485-495.

[4] Zhou C, Wu YL, Chen G, Feng J, Liu XQ, Wang C, Zhang S, Wang J, Zhou S, Ren S, Lu S, Zhang L, Hu C, Hu C, Luo Y, Chen L, Ye M, Huang J, Zhi X, Zhang Y, Xiu Q, Ma J, Zhang L and You C. Erlotinib versus chemotherapy as first-line treatment for patients with advanced EGFR mutation-positive non-small-cell lung cancer (OPTIMAL, CTONG-0802): a multicentre, open-label, randomised, phase 3 study. Lancet Oncol 2011; 12: 735-742.

[5] Rosell R, Carcereny E, Gervais R, Vergnenegre A, Massuti B, Felip E, Palmero R, Garcia-Gomez R, Pallares C, Sanchez JM, Porta R, Cobo M, Garrido P, Longo F, Moran T, Insa A, De Marinis F, Corre R, Bover I, Illiano A, Dansin E, De Castro J, Milella M, Reguart N, Altavilla G, Jimenez U, Provencio M, Moreno MA, Terrasa J, Munoz-Langa J, Valdivia J, Isla D, Domine M, Molinier O, Mazieres J, Baize N, Garcia-Campelo R, Robinet G, Rodriguez-Abreu D, Lopez-Vivanco G, Gebbia V, Ferrera-Delgado L, Bombaron P, Bernabe R, Bearz A, Artal A, Cortesi E, Rolfo C, Sanchez-Ronco M, Drozdowskyj A, Queralt C, De Aguirre I, Ramirez JL, Sanchez JJ, Molina MA, Taron M, Paz-Ares L; Spanish Lung Cancer Group in collaboration with Groupe Francais De Pneumo-Cancérologie and Associazione Italiana Oncologia T. Erlotinib versus standard chemotherapy as first-line treatment for European patients with advanced EGFR mutation-positive non-small-cell lung cancer (EURTAC): a multicentre, open-label, randomised phase 3 trial. Lancet Oncol 2012; 13: 239-246.

[6] Pao W, Miller VA, Politi KA, Riely GJ, Somwar R, Zakowski MF, Kris MG and Varmus H. Acquired

resistance of lung adenocarcinomas to gefitinib or erlotinib is associated with a second mutation in the EGFR kinase domain. PLoS Med 2005; 2: e73.

[7] Shigematsu H, Lin L, Takahashi T, Nomura M, Suzuki M, Wistuba II, Fong KM, Lee H, Toyooka S, Shimizu N, Fujisawa T, Feng Z, Roth JA, Herz J, Minna JD and Gazdar AF. Clinical and biological features associated with epidermal growth factor receptor gene mutations in lung cancers. J Natl Cancer Inst 2005; 97: 339-346.

[8] Sharma SV, Bell DW, Settleman J and Haber DA. Epidermal growth factor receptor mutations in lung cancer. Nat Rev Cancer 2007; 7: 169-181.

[9] Engelman JA and Janne PA. Factors predicting response to EGFR tyrosine kinase inhibitors. Semin Respir Crit Care Med 2005; 26: 314-322.

[10] Giaccone G. Epidermal growth factor receptor inhibitors in the treatment of non-small-cell lung cancer. J Clin Oncol 2005; 23: 3235-3242.

[11] Wang SE, Narasanna A, Perez-Torres M, Xiang B, Wu FY, Yang S, Carpenter G, Gazdar AF, Muthuswamy SK and Arteaga CL. HER2 kinase domain mutation results in constitutive phosphorylation and activation of HER2 and EGFR and resistance to EGFR tyrosine kinase inhibitors. Cancer Cell 2006; 10: 25-38.

[12] Prahallad A, Sun C, Huang S, Di Nicolantonio F, Salazar R, Zecchin D, Beijersbergen RL, Bardelli A and Bernards R. Unresponsiveness of colon cancer to BRAF(V600E) inhibition through feedback activation of EGFR. Nature 2012; 483: 100-103.

[13] Gusenbauer S, Vlaicu P and Ullrich A. HGF induces novel EGFR functions involved in resistance formation to tyrosine kinase inhibitors. Oncogene 2012; doi: 10.1038/onc.2012.396. [Epub ahead of print].

[14] Engelman JA, Zejnullahu K, Mitsudomi T, Song Y, Hyland C, Park JO, Lindeman N, Gale CM, Zhao X, Christensen J, Kosaka T, Holmes AJ, Rogers AM, Cappuzzo F, Mok T, Lee C, Johnson BE, Cantley LC and Janne PA. MET amplification leads to gefitinib resistance in lung cancer by activating ERBB3 signaling. Science 2007; 316: 1039-1043.

[15] Pao W and Girard N. New driver mutations in non-small-cell lung cancer. Lancet Oncol 2011; 12: 175-180.

[16] Cheng L, Alexander RE, Maclennan GT, Cummings OW, Montironi R, Lopez-Beltran A, Cramer HM, Davidson DD and Zhang S. Molecular pathology of lung cancer: key to personalized medicine. Mod Pathol 2012; 25: 347-369.

[17] Yauch RL, Januario T, Eberhard DA, Cavet G, Zhu W, Fu L, Pham TQ, Soriano R, Stinson J, Seshagiri S, Modrusan Z, Lin CY, O'Neill V and Amler LC. Epithelial versus mesenchymal phenotype determines in vitro sensitivity and predicts clinical activity of erlotinib in lung cancer patients. Clin Cancer Res 2005; 11: 8686-8698.

[18] Sos ML, Michel K, Zander T, Weiss J, Frommolt P, Peifer M, Li D, Ullrich R, Koker M, Fischer F, Shimamura T, Rauh D, Mermel C, Fischer S, Stuckrath I, Heynck S, Beroukhim R, Lin W, Winckler W, Shah K, LaFramboise T, Moriarty WF, Hanna M, Tolosi L, Rahnenfuhrer J, Verhaak R, Chiang D, Getz G, Hellmich M, Wolf J, Girard L, Peyton M, Weir BA, Chen TH, Greulich H, Barretina J, Shapiro GI, Garraway LA, Gazdar AF, Minna JD, Meyerson M, Wong KK and Thomas RK. Predicting drug susceptibility of non-small cell lung cancers based on genetic lesions. J Clin Invest 2009; 119: 1727-1740.

[19] Yao Z, Fenoglio S, Gao DC, Camiolo M, Stiles B, Lindsted T, Schlederer M, Johns C, Altorki N, Mittal V, Kenner L and Sordella R. TGF-beta IL-6 axis mediates selective and adaptive mechanisms of resistance to molecular targeted therapy in lung cancer. Proc Natl Acad Sci USA 2010; 107: 15535-15540.

[20] Frederick BA, Helfrich BA, Coldren CD, Zheng D, Chan D, Bunn PA Jr and Raben D. Epithelial to mesenchymal transition predicts gefitinib resistance in cell lines of head and neck squamous cell carcinoma and non-small cell lung carcinoma. Mol Cancer Ther 2007; 6: 1683-1691.

[21] Balko JM, Potti A, Saunders C, Stromberg A, Haura EB and Black EP. Gene expression patterns that predict sensitivity to epidermal growth factor receptor tyrosine kinase inhibitors in lung cancer cell lines and human lung tumors. BMC Genomics 2006; 7: 289.

[22] Yonesaka K, Zejnullahu K, Lindeman N, Homes AJ, Jackman DM, Zhao F, Rogers AM, Johnson BE and Janne PA. Autocrine production of amphiregulin predicts sensitivity to both gefitinib and cetuximab in EGFR wild-type cancers. Clin Cancer Res 2008; 14: 6963-6973.

[23] Petty WJ, Voelzke WR, Urbanic JJ, Varela VA, Waller LL, Swift CB, Graham RM, Memoli VA and Dragnev KH. High cyclin D3 expression confers erlotinib resistance in aerodigestive tract cancer. Lung Cancer 2011; 74: 384-391.

[24] Tusher VG, Tibshirani R and Chu G. Significance analysis of microarrays applied to the ionizing radiation response. Proc Natl Acad Sci USA 2001; 98: 5116-5121.

[25] McDermott U, Sharma SV, Dowell L, Greninger P, Montagut C, Lamb J, Archibald H, Raudales R, Tam A, Lee D, Rothenberg SM, Supko JG,

Sordella R, Ulkus LE, Iafrate AJ, Maheswaran S, Njauw CN, Tsao H, Drew L, Hanke JH, Ma XJ, Erlander MG, Gray NS, Haber DA and Settleman J. Identification of genotype-correlated sensitivity to selective kinase inhibitors by using high-throughput tumor cell line profiling. Proc Natl Acad Sci USA 2007; 104: 19936-19941.

[26] Xuan YT, Guo Y, Zhu Y, Wang OL, Rokosh G, Messing RO and Bolli R. Role of the protein kinase C-epsilon-Raf-1-MEK-1/2-p44/42 MAPK signaling cascade in the activation of signal transducers and activators of transcription 1 and 3 and induction of cyclooxygenase-2 after ischemic preconditioning. Circulation 2005; 112: 1971-1978.

[27] Li D, Lin HH, McMahon M, Ma H and Ann DK. Oncogenic raf-1 induces the expression of non-histone chromosomal architectural protein HMGI-C via a p44/p42 mitogen-activated protein kinase-dependent pathway in salivary epithelial cells. J Biol Chem 1997; 272: 25062-25070.

[28] Goh LL and Manser E. The RhoA GEF Syx is a target of Rnd3 and regulated via a Raf1-like ubiquitin-related domain. PLoS One 2010; 5: e12409.

[29] Cardoso AP, Pinto ML, Pinto AT, Oliveira MI, Pinto MT, Goncalves R, Relvas JB, Figueiredo C, Seruca R, Mantovani A, Mareel M, Barbosa MA and Oliveira MJ. Macrophages stimulate gastric and colorectal cancer invasion through EGFY Y, c-Src, Erk1/2 and Akt phosphorylation and smallGTPase activity. Oncogene 2013; doi:10.1038/onc.2013.154. [Epub ahead of print].

[30] Humtsoe JO and Kramer RH. Differential epidermal growth factor receptor signaling regulates anchorage-independent growth by modulation of the PI3K/AKT pathway. Oncogene 2010; 29: 1214-1226.

[31] Bivona TG, Hieronymus H, Parker J, Chang K, Taron M, Rosell R, Moonsamy P, Dahlman K, Miller VA, Costa C, Hannon G and Sawyers CL. FAS and NF-kappaB signalling modulate dependence of lung cancers on mutant EGFR. Nature 2011; 471: 523-526.

[32] Faber AC, Li D, Song Y, Liang MC, Yeap BY, Bronson RT, Lifshits E, Chen Z, Maira SM, Garcia-Echeverria C, Wong KK and Engelman JA. Differential induction of apoptosis in HER2 and EGFR addicted cancers following PI3K inhibition. Proc Natl Acad Sci USA 2009; 106: 19503-19508.

[33] Sos ML, Koker M, Weir BA, Heynck S, Rabinovsky R, Zander T, Seeger JM, Weiss J, Fischer F, Frommolt P, Michel K, Peifer M, Mermel C, Girard L, Peyton M, Gazdar AF, Minna JD, Garraway LA, Kashkar H, Pao W, Meyerson M and Thomas RK. PTEN loss contributes to erlotinib resistance in EGFR-mutant lung cancer by activation of Akt and EGFR. Cancer Res 2009; 69: 3256-3261.

[34] Wang YC, Kulp SK, Wang D, Yang CC, Sargeant AM, Hung JH, Kashida Y, Yamaguchi M, Chang GD and Chen CS. Targeting endoplasmic reticulum stress and Akt with OSU-03012 and gefitinib or erlotinib to overcome resistance to epidermal growth factor receptor inhibitors. Cancer Res 2008; 68: 2820-2830.

[35] Eiseler T, Kohler C, Nimmagadda SC, Jamali A, Funk N, Joodi G, Storz P and Seufferlein T. Protein kinase D1 mediates anchorage-dependent and -independent growth of tumor cells via the zinc finger transcription factor Snail1. J Biol Chem 2012; 287: 32367-32380.

[36] White GE, Tan TC, John AE, Whatling C, McPheat WL and Greaves DR. Fractalkine has anti-apoptotic and proliferative effects on human vascular smooth muscle cells via epidermal growth factor receptor signalling. Cardiovasc Res 2010; 85: 825-835.

[37] Tardaguila M, Mira E, Garcia-Cabezas MA, Feijoo AM, Quintela-Fandino M, Azcoitia I, Lira SA and Manes S. CX3CL1 promotes breast cancer via transactivation of the EGF pathway. Cancer Res 2013; [Epub ahead of print].

[38] Volin MV, Huynh N, Klosowska K, Chong KK and Woods JM. Fractalkine is a novel chemoattractant for rheumatoid arthritis fibroblast-like synoviocyte signaling through MAP kinases and Akt. Arthritis Rheum 2007; 56: 2512-2522.

[39] Ferretti E, Bertolotto M, Deaglio S, Tripodo C, Ribatti D, Audrito V, Blengio F, Matis S, Zupo S, Rossi D, Ottonello L, Gaidano G, Malavasi F, Pistoia V and Corcione A. A novel role of the CX3CR1/CX3CL1 system in the cross-talk between chronic lymphocytic leukemia cells and tumor microenvironment. Leukemia 2011; 25: 1268-1277.

[40] Jarboe JS, Dutta S, Velu SE and Willey CD. Mini-Review: Bmx Kinase Inhibitors for Cancer Therapy. Recent Pat Anticancer Drug Discov 2012; 8: 228-38.

[41] Hur W, Velentza A, Kim S, Flatauer L, Jiang X, Valente D, Mason DE, Suzuki M, Larson B, Zhang J, Zagorska A, Didonato M, Nagle A, Warmuth M, Balk SP, Peters EC and Gray NS. Clinical stage EGFR inhibitors irreversibly alkylate Bmx kinase. Bioorg Med Chem Lett 2008; 18: 5916-5919.

Supplementary data

Supplementary Table 1. Primers for qPCR validation

gene	forward	reverse
Actb	caccatgtaccctggcatt	gtacttgcgctcaggaggag
CCNT1	ACAACAAACGGTGGTATTTCACT	CCTGCTGGCGATAAGAAAGTT
CNNM4	CAGGAGATTCGCACTGTTTACAA	GGGCTCCGTCACCTTCAAC
CTNNA1	AAGCGAAGATTGCGGAACA	CATTTGGACACTTCAGCATCCA
CX3CL1	CCATGAGTCCCCTGTTTGTTTC	TGCCTACAACTTCCCCTTTCC
CXCL16	CAGAAGCAGCCGGAAAAAAAT	GGACTGGCACTGTGGCTGAT
CXCR4	ACGCCACCAACAGTCAGAG	AGTCGGGAATAGTCAGCAGGA
EGFR	TCTGCCGCAAATTCCGAGAC	GTGGGGTTGTAGAGCATGAGT
EPHB4	CCACCGGGAAGGTGAATGTC	CTGGGCGCACTTTTTGTAGAA
MYC	GGCGAACACACAACGTCTTG	TGGTCACGCAGGGCAAA
RAB3D	CACCATCACCACGGCCTACT	CGGCAAAGGATTCCTGATTG
RET	AAAGTGGCATTGGGCCTCTAC	GCAGGGCATGGACGTACAG
STK10	TCAGGAGTCCCACCTTGCAT	GCATTCCATTTCCCCCTGAT
TP53	CAGCACATGACGGAGGTTGT	TCATCCAAATACTCCACACGC

Supplementary Table 2. Significantly expression-altered genes in Calu-6 compared to U1752

Probe Set ID	Gene Symbol	Normalized difference	fold change	*P* value
8151532	FABP4	2.6974	6.486319	2.29E-03
8072626	TIMP3	2.6526	6.287995	6.80E-04
8047467	CDK15	2.4937	5.632206	3.55E-04
8108217	TGFBI	2.4842	5.59524	4.46E-04
7954090	EMP1	2.3863	5.228148	6.63E-04
7982597	THBS1	2.2967	4.913326	3.31E-05
8120967	NT5E	2.2249	4.674785	7.40E-06
7908388	RGS1	2.2249	4.674785	8.63E-04
8058857	IGFBP5	2.1317	4.382336	8.98E-04
8003667	SERPINF1	2.1011	4.290364	1.37E-03
8021081	SLC14A1	2.0958	4.274631	9.29E-04
8166611	MAGEB2	2.0954	4.273446	7.97E-04
7948229	SLC43A3	2.0428	4.120445	4.65E-05
8059905	COL6A3	2.0232	4.064844	3.43E-03
8102950	INPP4B	2.0215	4.060057	1.50E-03
7954196	MGST1	2.0159	4.044328	9.41E-04
8081548	PVRL3	2.013	4.036207	1.07E-04
8109677	GABRG2	1.992	3.977881	8.99E-04
7962579	AMIGO2	1.9752	3.931827	6.39E-04
8157524	TLR4	1.9164	3.774799	7.73E-03
7914270	LAPTM5	1.8676	3.64925	2.98E-04
8045664	LYPD6B	1.8387	3.576876	4.12E-05
8138381	AGR2	1.7371	3.333644	9.14E-03
8152512	TNFRSF11B	1.7184	3.290713	1.10E-02
7974341	GNG2	1.7124	3.277055	1.36E-03
8147000	ZFHX4	1.7074	3.265718	1.36E-03
8058765	FN1	1.6959	3.239789	1.17E-04

8140709	KIAA1324L	1.6903	3.227238	3.18E-03
8140967	SAMD9	1.6825	3.209837	2.02E-02
8129974	FUCA2	1.6594	3.158851	6.26E-04
8040365	TRIB2	1.6538	3.146614	6.82E-03
8113234	PCSK1	1.6491	3.136379	2.31E-04
8152606	SNTB1	1.6442	3.125745	4.46E-03
7983718	SCG3	1.6375	3.111262	5.74E-03
7947230	BDNF	1.636	3.108029	4.14E-03
7944351	FOXR1	1.6266	3.087844	3.07E-04
8100109	GABRA2	1.6191	3.071833	9.34E-06
8147030	STMN2	1.6173	3.068003	1.03E-03
8077899	PPARG	1.5784	2.986385	2.48E-05
8021169	LIPG	1.5772	2.983902	6.94E-04
7972713	EFNB2	1.5685	2.965962	1.36E-04
8104901	IL7R	1.5617	2.952015	9.35E-03
8078350	TGFBR2	1.553	2.934267	2.97E-03
8057506	FRZB	1.5393	2.906534	5.08E-03
7955613	KRT7	1.5239	2.875674	2.30E-02
8138745	HOXA7	1.5042	2.836673	2.33E-02
8051573	CDC42EP3	1.494	2.816688	6.65E-04
8095508	AMTN	1.4848	2.798784	9.02E-03
8036710	GMFG	1.4735	2.776948	3.70E-03
7972003	KLF12	1.4689	2.768108	3.06E-05
8106660	RASGRF2	1.4674	2.765231	9.85E-04
8018975	LGALS3BP	1.4653	2.761209	1.39E-03
8089082	DCBLD2	1.4594	2.74994	8.59E-04
8104663	CDH6	1.452	2.735871	2.91E-04
7922976	PTGS2	1.4476	2.727539	1.11E-03
7917912	DPYD	1.4436	2.719987	2.71E-04
8066822	SULF2	1.4386	2.710577	6.38E-04
7960362	LOC100128816	1.4257	2.686448	1.61E-03
8106448	PDE8B	1.4252	2.685517	4.69E-03
8068022	MIR155	1.42	2.675855	4.54E-03
8080810	PTPRG	1.4137	2.664196	2.98E-03
8115327	SPARC	1.402	2.642677	2.24E-04
7957140	LGR5	1.3987	2.636639	4.91E-03
8163637	TNC	1.3952	2.63025	6.95E-04
8128991	LAMA4	1.3901	2.620968	6.92E-03
8013753	RAB34	1.3877	2.616612	7.58E-03
8078330	RBMS3	1.3794	2.601602	3.76E-04
8150962	TOX	1.375	2.593679	4.99E-03
7955441	METTL7A	1.3749	2.593499	1.96E-03
7987145	FMN1	1.37	2.584706	6.69E-03
7939932	OR4C6	1.3451	2.540478	5.44E-04
8023415	TCF4	1.3405	2.532391	9.23E-05
8139500	TNS3	1.3394	2.530461	3.66E-04
8106743	VCAN	1.3354	2.523454	1.82E-03
8049487	MLPH	1.3335	2.520133	5.68E-04
7959856	PIWIL1	1.3247	2.504808	5.61E-03

7962559	SLC38A4	1.3179	2.49303	3.25E-03
8046078	B3GALT1	1.3152	2.488368	4.46E-03
8111387	ADAMTS12	1.3114	2.481823	1.25E-02
8140971	SAMD9L	1.3078	2.475637	1.90E-03
8138749	HOXA9	1.3063	2.473065	9.83E-04
8044212	SULT1C2	1.2943	2.45258	8.81E-04
8047738	NRP2	1.2886	2.442909	1.71E-03
8005171	TRPV2	1.285	2.436821	4.82E-04
7909789	TGFB2	1.2834	2.43412	1.37E-04
7902541	IFI44L	1.2824	2.432433	1.51E-02
7967325	HCAR1	1.2821	2.431927	1.87E-04
8175710	CSAG3	1.2683	2.408776	3.30E-03
8081431	ALCAM	1.2634	2.400608	3.18E-03
8103769	HPGD	1.2591	2.393464	3.69E-04
7995681	MMP2	1.2573	2.390479	2.59E-03
7944667	SORL1	1.2561	2.388492	6.38E-04
8114938	JAKMIP2	1.253	2.383365	2.56E-06
7986214	SLCO3A1	1.2481	2.375284	2.00E-03
8148040	MAL2	1.2412	2.363951	1.69E-03
8170576	CSAG1	1.2332	2.350879	3.64E-03
8111234	CDH12	1.2295	2.344857	1.39E-03
8150419	ZMAT4	1.2287	2.343557	9.84E-04
7920291	S100A16	1.2286	2.343395	4.51E-03
8150698	SNAI2	1.2282	2.342745	4.79E-04
7978407	PRKD1	1.2094	2.312414	2.45E-02
7908072	LAMC2	1.201	2.29899	1.85E-03
8150881	PLAG1	1.1972	2.292942	3.34E-02
8142981	PODXL	1.1907	2.282635	5.81E-04
8035304	BST2	1.1906	2.282476	2.98E-02
8170580	CSAG3	1.1855	2.274422	2.79E-03
8140955	CDK6	1.1836	2.271429	1.09E-04
8020973	FHOD3	1.1717	2.25277	3.41E-03
8095728	EREG	1.1699	2.249961	5.39E-05
8094789	LIMCH1	1.1609	2.235969	1.54E-03
7932985	NRP1	1.1593	2.23349	1.57E-03
7934979	ANKRD1	1.1553	2.227306	5.55E-04
7953321	LTBR	1.1546	2.226226	6.99E-03
8055688	RND3	1.1517	2.221755	1.31E-03
7956867	HMGA2	1.1514	2.221293	3.59E-04
8088776	FOXP1	1.1466	2.213915	4.11E-04
7957298	NAV3	1.1397	2.203352	2.48E-03
7985147	DNAJA4	1.1346	2.195577	3.80E-03
7951372	CASP4	1.1288	2.186768	1.03E-03
8018754	CYGB	1.1249	2.180864	4.85E-03
8099591	RN5S157	1.1248	2.180713	1.15E-02
8099633	PPARGC1A	1.1236	2.1789	1.42E-04
7969665	HS6ST3	1.1213	2.175429	1.11E-03
8060997	SPTLC3	1.1209	2.174826	2.57E-03
8007100	IGFBP4	1.1205	2.174223	1.70E-05

8093332	ZNF876P	1.1194	2.172566	2.02E-02
8113130	MCTP1	1.1192	2.172265	1.24E-02
7957338	SYT1	1.1183	2.17091	5.02E-05
8079217	ZNF35	1.1158	2.167151	1.62E-02
7939341	CD44	1.113	2.16295	9.63E-04
8081590	PHLDB2	1.1106	2.159354	1.84E-03
8047487	FZD7	1.1083	2.155915	2.94E-04
8052872	TGFA	1.1078	2.155167	4.15E-03
8166747	SYTL5	1.1063	2.152928	1.79E-03
8037079	ATP1A3	1.1043	2.149945	2.44E-04
7908409	RGS2	1.1036	2.148902	8.83E-05
8065071	FLRT3	1.1032	2.148307	3.35E-03
8045499	HNMT	1.097	2.139094	1.30E-03
7917754	BCAR3	1.0921	2.131841	8.69E-04
8039075	VN1R4	1.0881	2.125939	1.83E-02
8085797	THRB	1.0879	2.125644	4.55E-03
8013329	SNORD3D	1.0859	2.122699	4.37E-04
8013325	SNORD3B-2	1.0856	2.122258	4.39E-04
8013323	SNORD3B-1	1.0855	2.122111	4.38E-04
8005553	SNORD3B-2	1.0852	2.12167	4.38E-04
8005547	SNORD3D	1.0851	2.121523	4.38E-04
7905329	MLLT11	1.0827	2.117996	6.21E-04
8083594	PTX3	1.0809	2.115355	5.25E-03
7917944	MIR137	1.0715	2.101617	3.86E-02
8051864	LOC728819	1.0669	2.094927	1.48E-02
8108447	CXXC5	1.0662	2.093911	2.25E-04
8045674	LYPD6	1.0646	2.09159	1.99E-02
8172043	SRPX	1.0625	2.088548	5.92E-05
8059413	DOCK10	1.0512	2.072253	2.50E-02
7990555	NRG4	1.0492	2.069382	3.64E-05
8138741	HOXA6	1.0473	2.066658	1.84E-03
7973974	PAX9	1.0471	2.066372	1.50E-03
8069269	COL6A1	1.0467	2.065799	8.71E-04
8102342	ELOVL6	1.0421	2.059223	4.41E-04
7914342	FABP3	1.0405	2.05694	2.91E-03
8081564	CD96	1.0399	2.056085	3.72E-03
7986293	MCTP2	1.0396	2.055658	3.32E-04
7930498	ACSL5	1.0349	2.048972	1.59E-02
7950899	RAB38	1.032	2.044857	1.93E-03
8029006	AXL	1.0302	2.042307	2.45E-03
7962000	PTHLH	1.0294	2.041175	3.87E-03
8091972	MECOM	1.0256	2.035806	2.39E-03
8068633	B3GALT5	1.0207	2.028903	1.33E-02
8054479	MALL	1.0158	2.022024	1.93E-03
7929711	GOLGA7B	1.0138	2.019223	4.00E-02
8150988	ASPH	1.0134	2.018663	1.28E-04
8059580	DNER	1.0113	2.015727	2.58E-03
7982000	SNORD116-26	1.0095	2.013213	1.48E-02
7899627	TINAGL1	1.007	2.009728	2.81E-03

8162216	SHC3	1.0051	2.007083	6.91E-04
7930980	PPAPDC1A	1.0029	2.004024	2.44E-03
8145977	PLEKHA2	1.0026	2.003608	3.74E-04
8117422	HIST1H4F	-1.0015	0.49948	1.15E-02
8105908	OCLN	-1.0033	0.498858	5.86E-04
8142471	WNT2	-1.0089	0.496925	1.18E-02
7976836	MIR495	-1.0104	0.496409	3.85E-02
8048026	CPS1	-1.0164	0.494348	3.94E-03
8155864	RORB	-1.0183	0.493698	3.87E-04
7928994	LIPK	-1.0261	0.491036	5.76E-06
8148317	MYC	-1.0329	0.488727	4.49E-04
8163896	STOM	-1.0362	0.48761	1.21E-03
8091715	LXN	-1.0482	0.483571	9.21E-05
8140579	CACNA2D1	-1.049	0.483303	4.78E-05
8054297	CHST10	-1.05	0.482968	1.17E-02
8108378	CTNNA1	-1.0562	0.480897	2.09E-04
8081758	GRAMD1C	-1.0567	0.48073	1.34E-02
7918768	DENND2C	-1.0692	0.476583	4.45E-03
8075390	SEC14L4	-1.0693	0.47655	1.44E-02
8111255	CDH10	-1.0699	0.476352	4.77E-05
8005603	SLC47A1	-1.0746	0.474803	8.13E-03
7961215	STYK1	-1.0767	0.474112	1.33E-03
7932765	MPP7	-1.0818	0.472439	2.05E-03
8051583	CYP1B1	-1.083	0.472046	5.76E-04
7976073	FLRT2	-1.0866	0.47087	9.05E-03
7958200	EID3	-1.0872	0.470674	1.53E-03
8149825	STC1	-1.0901	0.469729	8.66E-05
7956878	IRAK3	-1.0902	0.469696	3.86E-04
8109938	RANBP17	-1.0906	0.469566	7.07E-03
8124534	HIST1H4L	-1.0915	0.469273	1.10E-03
8113103	KIAA0825	-1.0953	0.468039	5.35E-03
8075142	TTC28	-1.0954	0.468006	3.73E-04
7917276	LPAR3	-1.0977	0.467261	6.27E-03
8022692	DSC3	-1.1087	0.463712	2.36E-02
8149835	NEFL	-1.109	0.463615	7.53E-03
8076094	DMC1	-1.1096	0.463423	5.44E-03
8151931	TSPYL5	-1.1214	0.459648	2.55E-04
7960947	A2M	-1.1241	0.458788	1.19E-03
7964834	CPM	-1.1278	0.457613	8.36E-03
8036309	ZFP82	-1.1313	0.456504	2.18E-03
8174654	KLHL13	-1.1338	0.455714	1.28E-03
8091515	GPR87	-1.1345	0.455493	2.22E-02
8020164	GNAL	-1.136	0.455019	2.87E-04
7901460	GPX7	-1.1453	0.452096	1.28E-03
8062873	KCNK15	-1.1475	0.451407	2.58E-03
8169249	MID2	-1.1547	0.44916	1.42E-03
8066431	ADA	-1.1648	0.446026	1.88E-03
8111203	LOC285696	-1.1649	0.445995	4.09E-03
7954293	PDE3A	-1.1661	0.445624	5.28E-04

7991070	HDGFRP3	-1.1694	0.444606	5.28E-03
8173299	EDA2R	-1.1779	0.441994	2.92E-03
8149574	CSGALNACT1	-1.1783	0.441872	1.00E-03
8147796	RIMS2	-1.1855	0.439672	7.77E-03
7984704	NEO1	-1.1885	0.438759	4.62E-04
8108713	PCDHB8	-1.1963	0.436393	1.04E-02
8051298	GALNT14	-1.2016	0.434793	1.24E-03
8123920	ELOVL2	-1.2032	0.434311	5.90E-03
8068100	LINC00189	-1.2042	0.43401	8.27E-03
8011713	CXCL16	-1.205	0.433769	2.78E-02
8114354	NME5	-1.2056	0.433589	6.84E-03
7944803	VWA5A	-1.2078	0.432928	2.01E-04
8063458	DOK5	-1.208	0.432868	1.04E-03
8039054	ZNF347	-1.2092	0.432508	1.55E-03
8024712	ATCAY	-1.2102	0.432209	9.25E-04
8133728	ZP3	-1.2115	0.431819	3.18E-02
7898916	GRHL3	-1.2132	0.431311	2.61E-04
8081219	ST3GAL6	-1.2151	0.430743	3.74E-04
8073766	RIBC2	-1.2154	0.430654	1.38E-03
8107673	GRAMD3	-1.2192	0.429521	3.29E-04
8135661	CFTR	-1.2237	0.428183	2.49E-04
8022176	LAMA1	-1.2313	0.425933	1.94E-03
8113358	ST8SIA4	-1.2335	0.425284	3.14E-03
8089015	PROS1	-1.2447	0.421996	6.01E-03
8047788	ADAM23	-1.2581	0.418094	1.91E-03
8015412	JUP	-1.2591	0.417805	7.82E-04
8020384	GREB1L	-1.2615	0.41711	1.20E-02
8055952	NR4A2	-1.2634	0.416561	1.03E-04
8014248	SLFN13	-1.2668	0.415581	2.93E-03
8146738	MCMDC2	-1.275	0.413225	2.31E-03
8128553	BVES	-1.2751	0.413197	4.77E-03
8144742	EFHA2	-1.2792	0.412024	1.18E-03
8072229	NEFH	-1.2854	0.410257	3.44E-03
8121749	GJA1	-1.2879	0.409547	5.40E-04
8100870	ADAMTS3	-1.2897	0.409036	6.00E-03
7961440	PLBD1	-1.294	0.407819	1.77E-03
8096050	FGF5	-1.2985	0.406549	7.77E-04
8117045	RBM24	-1.301	0.405845	1.03E-03
8052399	BCL11A	-1.3066	0.404273	4.09E-03
8100338	ERVMER34-1	-1.3067	0.404244	3.09E-03
8116874	SYCP2L	-1.3186	0.400924	3.84E-03
8149927	CLU	-1.3291	0.398016	2.58E-04
8174598	IL13RA2	-1.3321	0.39719	7.62E-04
8141094	PDK4	-1.333	0.396942	8.05E-04
8096061	C4orf22	-1.3442	0.393872	2.38E-03
8099760	ARAP2	-1.3519	0.391776	2.42E-03
8104107	TRIML2	-1.3579	0.39015	2.14E-03
8122240	RN5S219	-1.3612	0.389258	5.57E-03
8173059	WNK3	-1.3673	0.387616	2.97E-03

8169186	TBC1D8B	-1.3733	0.386007	1.01E-02
8051762	SLC8A1	-1.3822	0.383633	4.46E-04
7965231	MGAT4C	-1.3823	0.383607	7.20E-03
7983478	C15orf48	-1.4026	0.378247	1.02E-02
8054135	MGAT4A	-1.4041	0.377854	5.10E-03
8175234	GPC3	-1.4092	0.37652	1.22E-03
8123315	QKI	-1.4101	0.376286	1.71E-02
8014233	SLFN11	-1.4146	0.375114	1.42E-03
8122150	EYA4	-1.4178	0.374283	3.42E-03
8111569	RANBP3L	-1.424	0.372678	2.79E-03
8031398	NLRP2	-1.427	0.371903	3.90E-03
7971077	POSTN	-1.4323	0.37054	7.70E-03
7901497	ZYG11A	-1.4335	0.370232	1.32E-02
7901720	PRKAA2	-1.4367	0.369411	1.04E-04
8127767	ELOVL4	-1.443	0.367802	1.10E-02
8123864	TFAP2A	-1.4518	0.365565	1.35E-03
8141066	PON3	-1.4522	0.365464	1.98E-03
8092169	TNFSF10	-1.4559	0.364528	1.63E-03
8098856	RNF212	-1.4599	0.363518	2.12E-04
8054281	LONRF2	-1.4684	0.361383	3.76E-04
8092251	GNB4	-1.4732	0.360183	1.68E-02
8056323	FIGN	-1.4817	0.358067	1.32E-03
8006433	CCL2	-1.4818	0.358042	2.66E-04
7943413	BIRC3	-1.483	0.357744	5.40E-04
8151341	TRPA1	-1.4885	0.356383	3.79E-03
8112007	EMB	-1.4991	0.353774	2.81E-03
8142079	EFCAB10	-1.5014	0.35321	5.91E-03
8083616	MLF1	-1.5048	0.352379	2.30E-02
8035813	ZNF43	-1.5054	0.352233	6.57E-03
7907222	PRRX1	-1.5115	0.350746	1.45E-04
8070632	CBS	-1.5179	0.349194	6.80E-04
7988414	GATM	-1.5273	0.346926	4.38E-03
7932453	NEBL	-1.5448	0.342743	2.54E-04
8094751	CHRNA9	-1.5464	0.342363	1.91E-03
8166314	PPEF1	-1.5553	0.340258	1.58E-03
8167701	XAGE1B	-1.5561	0.340069	1.19E-03
8167710	XAGE1A	-1.5562	0.340046	1.19E-03
8172757	XAGE1E	-1.5565	0.339975	1.19E-03
8083743	ARL14	-1.5684	0.337182	1.60E-03
8122365	GPR126	-1.5892	0.332356	7.32E-04
8104601	BASP1	-1.6077	0.328121	8.28E-04
8076704	SMC1B	-1.6131	0.326895	1.79E-05
8108697	PCDHB5	-1.6174	0.325922	9.23E-03
7910030	DNAH14	-1.636	0.321747	7.91E-03
8080847	C3orf14	-1.6458	0.319569	4.96E-04
8031632	ZNF542	-1.655	0.317538	6.00E-04
8022711	DSC2	-1.666	0.315126	6.67E-04
8083968	NLGN1	-1.6713	0.31397	1.14E-02
8056611	LRP2	-1.6966	0.308512	2.17E-03

8175539	LDOC1	-1.6995	0.307893	9.97E-04
7927827	MYPN	-1.7026	0.307232	4.16E-03
8144726	TUSC3	-1.7034	0.307062	1.29E-03
8124604	TRNAA46P	-1.7061	0.306487	4.80E-03
7926545	PLXDC2	-1.7085	0.305978	2.30E-05
8135697	ANKRD7	-1.727	0.302079	4.24E-04
8052355	EFEMP1	-1.7591	0.295432	8.81E-03
8094778	UCHL1	-1.7683	0.293554	9.12E-04
8052438	LOC339803	-1.7751	0.292174	2.08E-02
8098379	WDR17	-1.8297	0.281323	7.45E-04
7957452	ALX1	-1.8515	0.277104	7.14E-04
8150138	TEX15	-1.8548	0.276471	1.96E-04
8140556	HGF	-1.8902	0.26977	9.05E-05
8067903	USP25	-1.936	0.26134	9.69E-05
7934215	SPOCK2	-1.9485	0.259085	1.22E-04
7903227	PALMD	-1.9585	0.257296	3.43E-04
8007643	C17orf104	-1.9625	0.256583	8.34E-04
8127502	LINC00472	-1.9658	0.255997	4.68E-05
8113773	ALDH7A1	-1.9826	0.253033	8.97E-03
7937079	BNIP3	-1.9953	0.250816	4.94E-05
8170531	MAGEA4	-2.0525	0.241066	2.53E-03
7962250	CPNE8	-2.0745	0.237418	5.26E-03
7944769	GRAMD1B	-2.0779	0.236859	7.15E-04
8124531	HIST1H3I	-2.0804	0.236449	4.36E-04
7922994	FAM5C	-2.1145	0.230926	1.93E-04
8069532	HSPA13	-2.2188	0.21482	4.90E-04
8105040	OSMR	-2.2762	0.206441	1.59E-03
7957458	NTS	-2.4193	0.186947	1.88E-04
8067140	CYP24A1	-2.4803	0.179207	1.88E-05
7930208	INA	-2.503	0.176409	7.36E-04
8112980	EDIL3	-2.6215	0.162499	7.84E-04
8141016	TFPI2	-3.1938	0.109287	5.08E-06

Supplementary Table 3. 13 genes regulated by RAF1

Probe ID	Genes in dataset	Prediction (based on expression direction)	Fold Change	Findings
7954090	EMP1	Activated	5.228	Upregulates
7908388	RGS1	Activated	4.675	Upregulates
8089082	DCBLD2	Activated	2.750	Upregulates
7922976	PTGS2	Activated	2.728	Upregulates
7934979	ANKRD1	Activated	2.227	Upregulates
8055688	RND3	Affected	2.222	Regulates
7956867	HMGA2	Activated	2.221	Upregulates
7939341	CD44	Activated	2.163	Upregulates
7962000	PTHLH	Activated	2.041	Upregulates
8105908	OCLN	Activated	-2.005	Downregulates
8148317	MYC	Inhibited	-2.046	Upregulates
8105040	OSMR	Inhibited	-4.844	Upregulates
8141016	TFPI2	Inhibited	-9.150	Upregulates